

Searches for BSM physics in diphoton final state at CMS

Milena Quittnat* on behalf of the CMS collaboration

ETH Zuerich

E-mail: milena.quittnat@cern.ch

Many physics scenarios beyond the standard model predict the existence of heavy resonances decaying to diphotons. This note presents searches for BSM physics performed on 3.3 fb^{-1} of proton-proton collision data collected by the CMS experiment in 2015 at a center-of-mass energy of 13 TeV. The interpretation of the search results focuses on spin-0 and spin-2 resonances in the mass range of 500 - 4500 GeV and with a relative width up to 5.6×10^{-2} . The results of the search at 13 TeV is combined with similar searches of the CMS experiment at $\sqrt{s} = 8 \text{ TeV}$ with 19.7 fb^{-1} of proton-proton collision data.

*XXIV International Workshop on Deep-Inelastic Scattering and Related Subjects
11-15 April, 2016
DESY Hamburg, Germany*

*Speaker.

Introduction

The resonant production of high mass diphoton pairs is predicted by several extensions of the standard model (SM) of particle physics. The spin of a resonance decaying to two photons must be either 0 or an integer greater than or equal to 2 [1, 2]. Spin-0 resonances decaying to two photons are predicted by SM extensions with non-minimal Higgs sectors [3], while spin-2 resonances decaying to two photons are motivated by models with additional space-like dimensions, namely the Randall-Sundrum (RS) graviton model [4]. With a new center-of-mass energy of $\sqrt{s} = 13$ TeV, the ATLAS [5] and CMS [6] collaborations recently presented results on searches for diphoton resonances in the mass ranges $200\text{ GeV} - 2\text{ TeV}$ and $500\text{ GeV} - 4.5\text{ TeV}$, respectively. The CMS collaboration combined their result on the $\sqrt{s} = 13$ TeV dataset statistically with those from similar searches performed at $\sqrt{s} = 8$ TeV. This note summarizes these results, published in Ref. [7, 8].

Event selection and reconstruction

A detailed description of the CMS detector, together with the relevant kinematic variables, can be found in Ref. [9] and a description of the used simulation sample in Ref. [8]. Photons are reconstructed by clustering spatially correlated energy deposits in the electromagnetic calorimeter (ECAL), the calibrations, corrections and techniques used are described in Ref. [10]. For the 13 TeV dataset and with a respective magnetic field of $B = 3.8\text{ T}$ ($B = 0\text{ T}$), the trigger selection requires at least two photon candidates of transverse momentum above 60 (40) GeV and is fully efficient for the search range of $m_X > 0.5\text{ TeV}$ [7]. In the search region for the 3.8 T dataset, the interaction vertex is correctly assigned for about 90% of the signal events [8]. Due to a different vertex algorithm for the $B = 0\text{ T}$ dataset, the probability for the correct assignment is only about 60%. Residual differences in the photon energy scale and resolution between data and simulation are determined and corrected for using $Z \rightarrow e^+e^-$ events, the procedure is described in Ref. [10]. The energy scale correction factors measured for the $B = 0\text{ T}$ dataset are found to be about 1% higher than the $B = 3.8\text{ T}$ factors. The resolution corrections are however similar. The variation of the corrections is studied with $Z \rightarrow e^+e^-$ events as a function of the transverse momentum p_T up to 150 or 100 GeV, respectively, for the central ECAL region (barrel) and the forward ECAL region (endcaps). The variation is smaller than 0.5 (0.7)% for EB (EE) in both datasets. The identification and trigger efficiencies agree within their uncertainties with the Monte-Carlo prediction. In each event, photon candidates are required to have a transverse momentum of $p_T > 75\text{ GeV}$ and a pseudorapidity of $|\eta_{SC}| < 2.5$ as well as $|\eta_{SC}| < 1.44$ for at least one of them. The invariant mass $m_{\gamma\gamma}$ of the pair is required to be above 230 GeV for events in which both photon are centrally detected (“EBEB”) and 320 GeV for events in which one photon is detected in the endcaps (“EBEE”). Photon candidates are further required to satisfy different sets of identification criteria, which are detailed in Ref. [8], depending on whether the data was recorded at $B = 3.8\text{ T}$ or at $B = 0\text{ T}$. In the $B = 3.8\text{ T}$ dataset, the efficiency of the identification criteria for prompt isolated photon candidate is above 90 (85)% in the barrel (endcaps). In the $B = 0\text{ T}$ dataset, the identification efficiency is above 85 (70)% for prompt isolated photon candidates in the barrel (endcaps). For the 3.8 (0) T analysis, the overall signal selection efficiency varies between 0.5-0.7 (0.4-0.5), depending on the signal hypothesis. Because of the different angular distribution of the decay products, for $m_X < 1\text{ TeV}$, the kinematic acceptance for the RS graviton resonances is approximately 20% lower than for scalar resonances. The two acceptances become similar for $m_X > 3\text{ TeV}$. About 90 (80)% of the

background events in the EBEB (EBEE) sample originate from the $\gamma\gamma$ -process. This Monte-Carlo prediction is validated in data for the 3.8 T analysis and is described in Ref. [7].

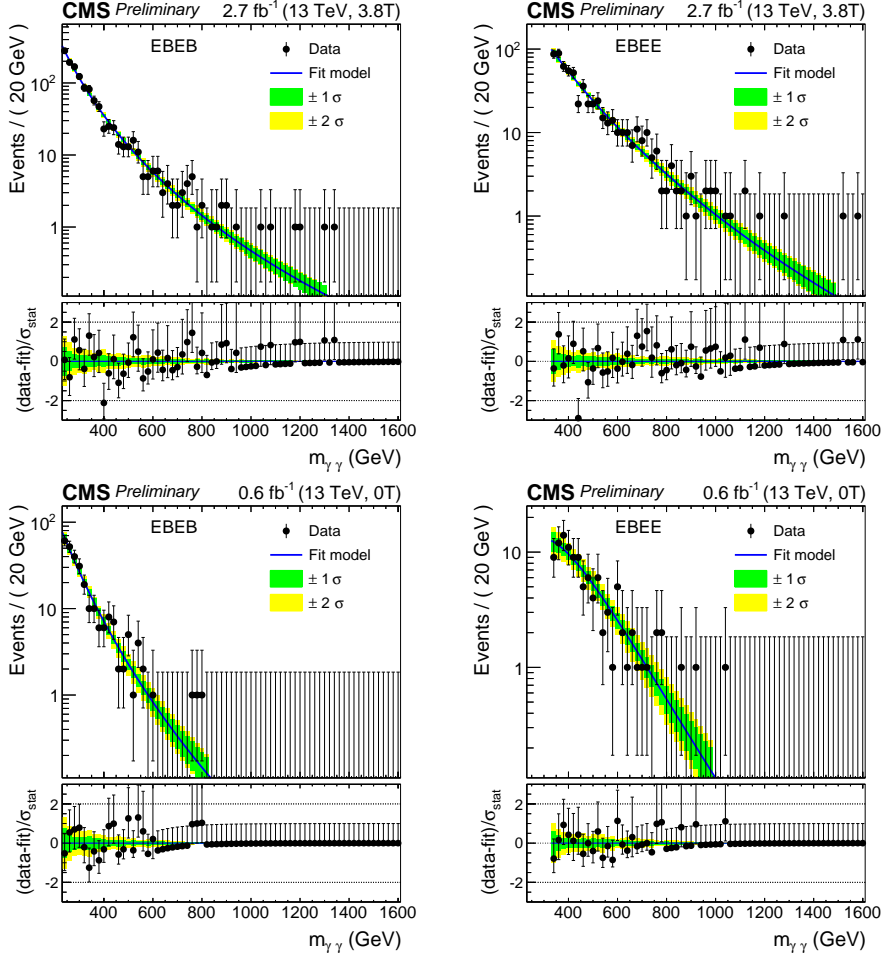


Figure 1: The observed invariant mass spectra are shown for the EBEB (left) and EBEE category (right). The top (bottom) row shows the results for the $B = 3.8\text{T}$ ($B = 0\text{T}$) dataset. The results of the parametric fits to the data are depicted with their uncertainties.

Diphoton mass spectrum and statistical analysis

The $m_{\gamma\gamma}$ distributions of the events selected by the 13 TeV analysis are shown in Fig. 1. The results of this search are interpreted using a composite statistical hypothesis test [7]. A simultaneous fit to the invariant mass spectra of the four EBEB, EBEE and $B = 3.8\text{T}$, $B = 0\text{T}$ event categories is used to study the compatibility of the data with the background-only and the signal+background hypotheses as described in Ref. [8]. The signal distribution in $m_{\gamma\gamma}$ is determined from the convolution of the intrinsic shape of the resonance and the ECAL detector response. In order to determine the signal normalisation, the efficiency of the final event selection is combined with the kinematic acceptance. The background $m_{\gamma\gamma}$ spectrum is described by a parametric function of $m_{\gamma\gamma}$. The parametric coefficients are obtained from a fit to the data events, and considered as unconstrained nuisance parameters in the hypothesis test, allowing a data-driven description of the shape. The

uncertainty on the accuracy of the background determination is assessed by a bias term [8] and accounted for in the hypothesis test. All uncertainties are evaluated independently for each of the four analysis categories and are assumed to be uncorrelated. In this analysis, the statistical uncertainties dominate over the systematic ones.

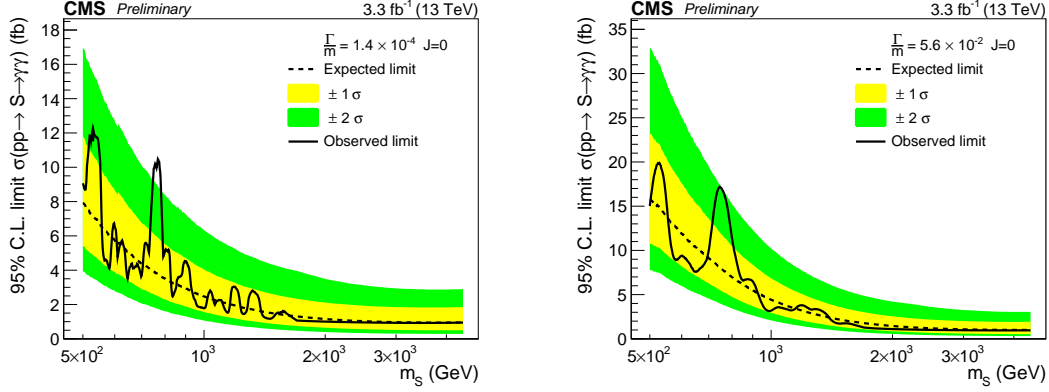


Figure 2: Expected and observed 95% C.L. exclusion limits in the range $500\text{ GeV} < m_X < 4.5\text{ TeV}$ for $\Gamma/m = 1.4 \times 10^{-4}$ (left) and 5.6×10^{-2} (right) for the scalar ($J=0$) resonance hypothesis.

Results of the search at $\sqrt{s} = 13$ TeV and combined analysis of $\sqrt{s} = 8$ TeV and 13 TeV datasets

The search range of a resonance mass m_X in the mass region $500\text{ GeV} < m_X < 4.5\text{ TeV}$ is interpreted for three values of relative width: $\Gamma/m = 0.14 \times 10^{-4}$, 0.14×10^{-2} and 5.6×10^{-2} . For the RS graviton model, where $\Gamma/m = 1.4\tilde{\kappa}^2$ [11], this corresponds to dimensionless coupling values of $\tilde{\kappa} = 0.01, 0.1$ and 0.2 . To set upper limits on the resonant diphoton production rate, the modified frequentist method, also known as CL_s , and asymptotic formulas are applied [8]. Expected and observed upper limits on the production of scalar and RS graviton resonances are shown in Fig. 2 for values Γ/m of 1.4×10^{-4} and 5.6×10^{-2} . The results for all signal hypotheses can be found in Ref. [7]. The compatibility of the observation with the background-only hypothesis is evaluated computing the background-only p -value, also known as the “local p -value” p_0 and depicted in Figure 3. The largest excess observed in data has a local significance of 2.9 standard deviations under the RS graviton hypothesis with a relative width of $\Gamma/m = 1.4 \times 10^{-2}$ and a mass of $m_G = 760\text{ GeV}$. The probability of observing at least one excess more significant than this in the mass range between 500 GeV and 4.5 TeV and among all considered hypotheses of this analysis, is called the “look-elsewhere-effect”. It is derived from a sampling distribution of $\max(p_0)$ of an ensemble of background-only pseudo datasets and found to be less than one standard deviation. The results of the $\sqrt{s} = 13$ TeV dataset is combined statistically with the results at $\sqrt{s} = 8$ TeV of the CMS collaboration, with an integrated luminosity of 19.7 fb^{-1} . Two analyzes were performed using the 8 TeV dataset: the analysis described in Ref. [12] searched for diphoton resonances in the mass range between 150 and 850 GeV under the spin-0 and spin-2 hypotheses, the analysis described in Ref. [13] focused on the mass range above 500 GeV and only on the spin-2 hypothesis. Since the event samples partially overlap, the analysis leading to the most stringent median expected exclusion limit on resonant diphoton production is evaluated at each m_X and is subsequently taken for the combination. The results of Ref. [12] are thus considered for $m_X < 850\text{ GeV}$ and those

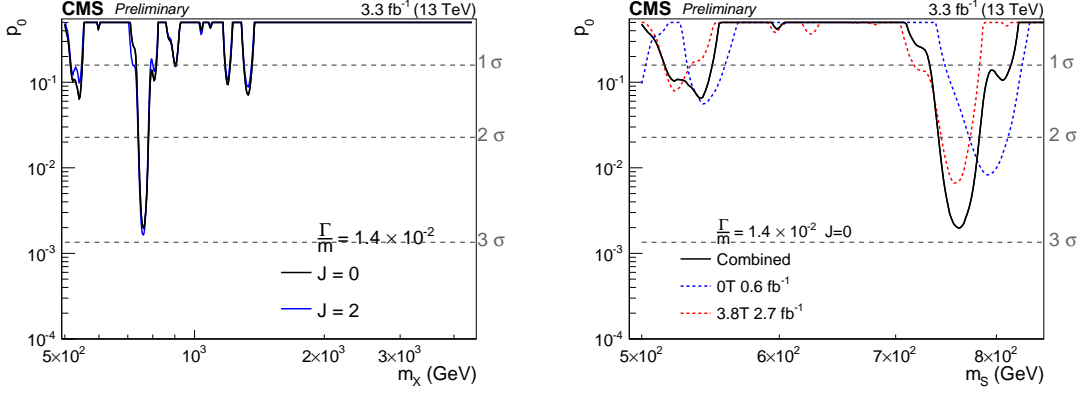


Figure 3: Observed background only p -values obtained on the 13 TeV dataset. For $\Gamma/m = 1.4 \times 10^{-2}$, the range $500 \text{ GeV} < m_X < 4.5 \text{ TeV}$ (850 GeV) is shown on the left (right). Results corresponding to both spin hypotheses are shown on the left. The contributions of the $B = 3.8 \text{ T}$ and $B = 0 \text{ T}$ datasets are shown separately on the right for $J=0$. Due to the different integrated luminosity, the weight of the $B = 0 \text{ T}$ dataset at $m_X = 760 \text{ GeV}$ is approximately 20 % of the $B = 3.8 \text{ T}$ one in the combined result.

of Ref. [13] for $m_X > 850 \text{ GeV}$. The ratio of the signal production cross sections at $\sqrt{s} = 8 \text{ TeV}$ and 13 TeV has been calculated [8]. It is approximately 0.29 (0.27) for $m_G(m_S) = 500 \text{ GeV}$, 0.24 (0.22) for $m_G(m_S) = 750 \text{ GeV}$ and decreases to approximately 0.04 (0.03) for masses in the TeV range (m_G or $m_S = 3 \text{ TeV}$). Further details of the statistical combination can be found in Ref. [8]. In the combined analysis, a simultaneous fit to the $m_{\gamma\gamma}$ spectra in all the event categories is performed, assuming a common signal strength modifier for all categories. Upper limits are set using the CL_s method. Background-only p -values are computed as described for the 13 TeV only dataset. The expected and observed median 95% C.L. exclusion limits on the equivalent 13 TeV production cross section, $\sigma_{G,S}^{13\text{TeV}} \cdot \mathcal{B}_{\gamma\gamma}$, for the combined analysis are shown on the left side of Figure 4. The combined analysis improves the exclusion limits by 20-40% for masses $< 1.5 \text{ TeV}$ with respect to the 8 or 13 TeV only datasets. For masses above 1.5 TeV, the exclusion limits are mainly driven by the sensitivity of the 13 TeV analysis. The local significance for the combined analysis is shown on the right side of Figure 4 under the narrow width scalar resonance hypothesis. This hypothesis shows the largest excess among all considered signal hypotheses with a local significance of roughly 3.4 standard deviations at a mass of $m_S = 750 \text{ GeV}$. At this mass, both datasets contribute with similar weights to the combined result. Further results can be found in Ref. [7]. The global significance of the excess, considering all tested signal hypotheses of the analysis, is estimated to be roughly 1.6 standard deviations [8].

In summary

This note summarizes the search for new physics in the diphoton final state by the CMS experiment [7, 8]. The analysis is performed on 3.3 fb^{-1} and 19.7 fb^{-1} of proton-proton collisions with a center-of-mass energy of $\sqrt{s} = 13 \text{ TeV}$ and $\sqrt{s} = 8 \text{ TeV}$, respectively. Limits on the production of scalar resonances ($J=0$) and RS gravitons ($J=2$) for resonance masses between $500 \text{ GeV} < m_X < 4.5 \text{ TeV}$ and $1.4 \times 10^{-4} < \Gamma/m < 5.6 \times 10^{-2}$ are determined. Using leading-order cross sections for RS graviton production, RS gravitons with masses below approximately

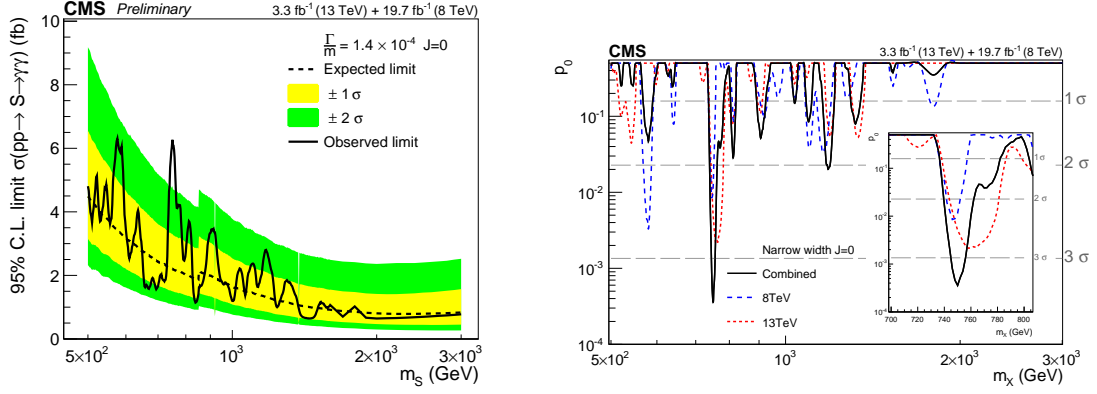


Figure 4: Left: upper limit on the narrow width for the production of high mass diphoton resonances obtained with the combined analysis of the 8 and 13 TeV data for $J=0$. Right: corresponding observed background only p-values, the contributions of the 8 and 13 TeV datasets are shown separately for $J=0$. At $m_X = 750$ GeV, both datasets add a similar weight to the combination.

1.6, 3.3, and 3.8 TeV are excluded at a 95% confidence level for $\tilde{\kappa} = 0.01, 0.1$, and 0.2 , respectively, corresponding to $\Gamma/m = 1.4 \times 10^{-4}, 1.4 \times 10^{-2}$ and 5.6×10^{-2} . A modest excess of events over the background-only hypothesis is observed for $m_X = 750$ GeV. The local significance under the narrow-width scalar resonance hypothesis of $\Gamma/m = 1.4 \times 10^{-4}$ is approximately 3.4 standard deviations. The global significance of the excess is 1.6 standard deviations, considering all signal hypotheses of this analysis. A larger dataset is required to determine the origin of this excess.

References

- [1] L.D. Landau, *Dokl. Akad. Nauk SSSR* **60** (1948) 207, [doi:10.1016/B978-0-08-010586-4.50070-5].
- [2] C.N. Yang, *Phys. Rev.* **77** (1950) 242, [doi:10.1103/PhysRev.77.242].
- [3] G. C. Branco et al., *Phys. Rept.* **516** (2012), [hep-ph/1106.0034].
- [4] L. Randall and R. Sundrum, *Phys. Rev.* **83** (1999) 3370, hep-ph/9905221.
- [5] ATLAS Collaboration, ATLAS-CONF-2015-081, <http://cds.cern.ch/record/2114853>.
- [6] CMS Collaboration, CMS-PAS-EXO-15-004, <https://cds.cern.ch/record/2114808>.
- [7] CMS Collaboration, CMS-PAS-EXO-16-018, <http://cds.cern.ch/record/2139899>.
- [8] V. Khachatryan et al. [CMS Collaboration], CERN-EP-2016-154, [hep-ex/1606.04093].
- [9] S. Chatrchyan et al. [CMS Collaboration], *JINST* **3** (2008) S08004, [doi:10.1088/1748-0221/3/08/S08004].
- [10] V. Khachatryan et al. [CMS Collaboration], *JINST* **10** (2015) P08010, physics.ins-det/1502.02702.
- [11] H. Davoudias et al, *Phys. Rev. Lett.* **84** (2000) 2080, [hep-ph/9909255].
- [12] V. Khachatryan et al. [CMS Collaboration], *Phys. Lett.* **B750**(2015)494-519, hep-ex/1506.02301.
- [13] CMS Collaboration, CMS-PAS-EXO-12-045, <http://cds.cern.ch/record/2017806>.